frontiers in Marine Science

ORIGINAL RESEARCH
published: 20 August 2020
doi: 10.3389/fmars.2020.00675

Influence of Algal Production and Decomposition on the Carbon Isotope Signature of Labile Particulate Organic Matter on a Productive Continental Shelf Under the Stress of Coastal Hypoxia

*Zixiang Yang[1,2], Han Zhang[3], Peihong Kang[1,2], Yangyang Zhao[1,2] and Tiantian Tang[1,2]**

[1] State Key Laboratory of Marine Environmental Science, Xiamen University, Xiamen, China, [2] College of Ocean and Earth Sciences, Xiamen University, Xiamen, China, [3] Key Laboratory of Urban Environment and Health, Institute of Urban Environment, Chinese Academy of Sciences, Xiamen, China

OPEN ACCESS

Edited by:
Stuart Wakeham,
University of Georgia, United States

Reviewed by:
Ying Wu,
East China Normal University, China
Hilary G. Close,
University of Miami, United States

***Correspondence:**
Tiantian Tang
tiantian.tang@xmu.edu.cn

Specialty section:
This article was submitted to Marine Biogeochemistry, a section of the journal Frontiers in Marine Science

Received: 29 February 2020
Accepted: 24 July 2020
Published: 20 August 2020

Citation:
Yang Z, Zhang H, Kang P, Zhao Y and Tang T (2020) Influence of Algal Production and Decomposition on the Carbon Isotope Signature of Labile Particulate Organic Matter on a Productive Continental Shelf Under the Stress of Coastal Hypoxia. Front. Mar. Sci. 7:675. doi: 10.3389/fmars.2020.00675

To better understand the sources and recycling of labile organic matter in coastal water, we studied the carbon isotope signature of particulate organic carbon (POC) and particulate amino acids, a major group of labile organic compounds, on the shelf of the northern South China Sea. In addition, we were able to compare effects of hypoxia on labile organic matter at one station on the shelf. We found that carbon-weighted average $\delta^{13}C$ values of particulate amino acids (*w*AA$\delta^{13}C$) were generally higher at more productive offshore stations than nearshore stations. This amino acid $\delta^{13}C$ distribution suggests that the labile fraction of organic matter in coastal water originated primarily from local primary production. In contrast, bulk POC $\delta^{13}C$ (PO^{13}C) values showed little spatial variation on the NSCS shelf. The different patterns of *w*AA$\delta^{13}C$ and PO^{13}C distributions indicate a combined effect of POM lability and physical processes on the isotopic distribution of organic materials on this productive shelf. Moreover, the amino acid $\delta^{13}C$ in coastal hypoxic water suggests local primary production as the most likely source of labile organic matter that drives hypoxia on the NSCS shelf. No clear difference was observed in particulate amino acid $\delta^{13}C$ distribution between hypoxic and oxic waters.

Keywords: hypoxia, continental shelf, labile organic carbon, amino acids, compound specific isotope analysis (CSIA)

INTRODUCTION

Usually, algal organic carbon is depleted in ^{13}C relative to its inorganic carbon source, i.e., dissolved CO_2 in seawater (Freeman, 2001). This RuBisCo catalyzed isotope fractionation has a linear relationship with the ratio of growth rate (μ) over [CO_2] (μ/[CO_2], Laws et al., 1995; Popp et al., 1998; Burkhardt et al., 1999). The carbon fixed by cells is used to synthesize biomolecules

through diverse metabolic pathways, which results in intracellular isotope fractionations among biomolecules (Hayes, 2001). Thus, carbon isotope signatures of individual organic compounds are determined by the inorganic carbon source, the RuBisCo catalyzed isotope fractionation, and the intracellular isotope fractionation that occurs during compound synthesis.

Amino acids (AA) are a major class of cellular compounds in algae. In the marine environment, AA are considered to be a biomarker of labile organic carbon because AA can be preferentially decomposed (Wakeham et al., 1997; Benner and Amon, 2015; Wakeham and Lee, 2019). The rapid development of compound specific isotopic analysis of individual AA has provided a new tool to investigate geochemical behavior of these labile organic carbon compounds (Close, 2019). AA carbon isotopes are used to determine the metabolic origins of organic matter from terrestrial organisms, microalgae, bacteria, even the same species grown in different metabolic patterns (Larsen et al., 2009, 2013, 2015; Tang et al., 2017b). In marine environments, the carbon isotope ratios of AA are subject to decompositional modification. Bacterial reworking of AA carbon isotopes has been identified in estuarine sediments, particles, and dissolved organic matter (Keil et al., 2001; McCarthy et al., 2004; Hannides et al., 2013). However, there is little information on the AA carbon isotope distribution in productive coastal oceans, particularly in areas under the stress of coastal hypoxia. Hypoxic waters have microbial communities and metabolisms that are very different from those of oxic seawater (e.g., Liu et al., 2017). We don't presently know how AA carbon isotopes respond to the characteristic hypoxic metabolism found in coastal environment.

The ocean, particularly the coastal ocean, has experienced a decline in oxygen concentrations and an increase of hypoxia (usually defined as DO <2 mg L^{-1}, or <65 μmol kg^{-1}) over the past century, primarily due to anthropogenic activity (Breitburg et al., 2018). Both natural and anthropogenic terrestrial sources bring abundant nutrients and organic carbon into coastal waters; decomposition of both terrestrial organic matter and the organic matter formed during local primary production can lower oxygen concentrations (Kemp et al., 1992; Rabalais et al., 2014). More frequent summer hypoxia has been documented on the shallow shelf of the northern South China Sea (NSCS) due to increasing loading of nutrients and organic carbon from the adjacent Pearl River system (Su et al., 2017; Lu et al., 2018; Zhao et al., 2020). Even though hypoxia is related to the remineralization of excess organic carbon, not all organic matter can be quickly or easily remineralized because of the varying reactivity and bioavailability of the organic compounds that make up organic matter (Benner and Amon, 2015). AA and other labile organic compounds can be easily decomposed into CO_2. Therefore, accumulation and subsequent decomposition of labile organic matter can effectively cause hypoxia in a short time. Labile organic carbon on the NSCS shelf comes mainly from two sources: *in situ* growth of phytoplankton on the shelf (Zhang and Li, 2010) and discharge from the Pearl River. The relative contribution of these two sources to the spreading summer hypoxia at the mouth of the Pearl River Estuary (PRE) is currently not clear.

Here we used AA carbon isotope signatures (AA $\delta^{13}C$) in particulate matter to investigate the sources and recycling of labile organic carbon in coastal waters along a transect across the inner shelf of the NSCS in the summer of 2018. At this time, oxygen concentrations were generally lower in bottom waters, but bottom hypoxia was observed at one site near the transect. After a tropical storm passed through our study area, we revisited that station, which had been replenished with oxygen, so that a comparison between hypoxic and oxic conditions was possible. Below, we present the general distribution of carbon isotope signatures of particulate AA and organic carbon along the transect, which provides the first set of information on isotopic geochemistry of labile organic carbon on this productive shelf system.

MATERIALS AND METHODS

Sample Collection

During a cruise on the R/V Haike 68, a transect across the inner NSCS shelf was surveyed seaward from the mouth of the PRE on July 12, 2018 (station information are shown in **Figure 1** and **Supplementary Table 1**). All sampling from Sta. A8–A14 was taken within a 14-h period while tidal movement was offshore. Water samples were collected from the surface (S, 1 m) and bottom (B, 12–25 m) of the water column using a Niskin Rosette sampler with a CTD profiler attached. Water samples were also collected beneath the surface mixed layer (M, 7–15 m) where temperature and salinity profiles showed strong stratification. Bottom hypoxia had been observed at station F303 (F303H) near transect A on July 11, 2018. The cruise was interrupted by Tropical Storm Son-Tinh which landed on Hainan Island on July 18, 2018. After the storm, we resampled Sta. F303 (F303O) on July 19, when the bottom water had been replenished with oxygen.

Particulate matter was collected by filtering the water samples of about 1 L through precombusted GFF filters, and then storing them at −20°C. Two filters were collected for each water sample, one for bulk organic carbon analysis, the other for compound specific analysis of AA. Salinity, temperature and bottle depth were provided by a CTD profiler (SBE21, Seabird). The concentrations of dissolved oxygen were measured on board by the Winkler method (Pai et al., 1993). The chl*a* concentrations were measured by a fluorometer after extracting filters with acetone.

Bulk Organic Carbon Concentrations and Bulk $PO^{13}C$ Values

Bulk organic carbon concentration on filters was analyzed following the method of Kao et al. (2012). Before analysis of bulk $PO^{13}C$, filters were dried overnight at 60°C and acidified with drops of 1 N HCl to remove any carbonate. The acidified filters were dried again overnight at 60°C, and placed in precombusted nickel cups. Organic carbon on the filters was converted to CO_2 on an Elemental analyzer (EA, Isoprime 500). The $^{13}CO_2/^{12}CO_2$ ratios were measured by coupled isotopic ratio mass spectrometry (EA-IRMS, Isoprime 500). The stable isotope standards glutamic acid (USGS-40) and acetanilide (Merck) were used to calibrate the $\delta^{13}C$ ratios and concentrations of bulk organic carbon samples, with a standard deviation of 0.09‰

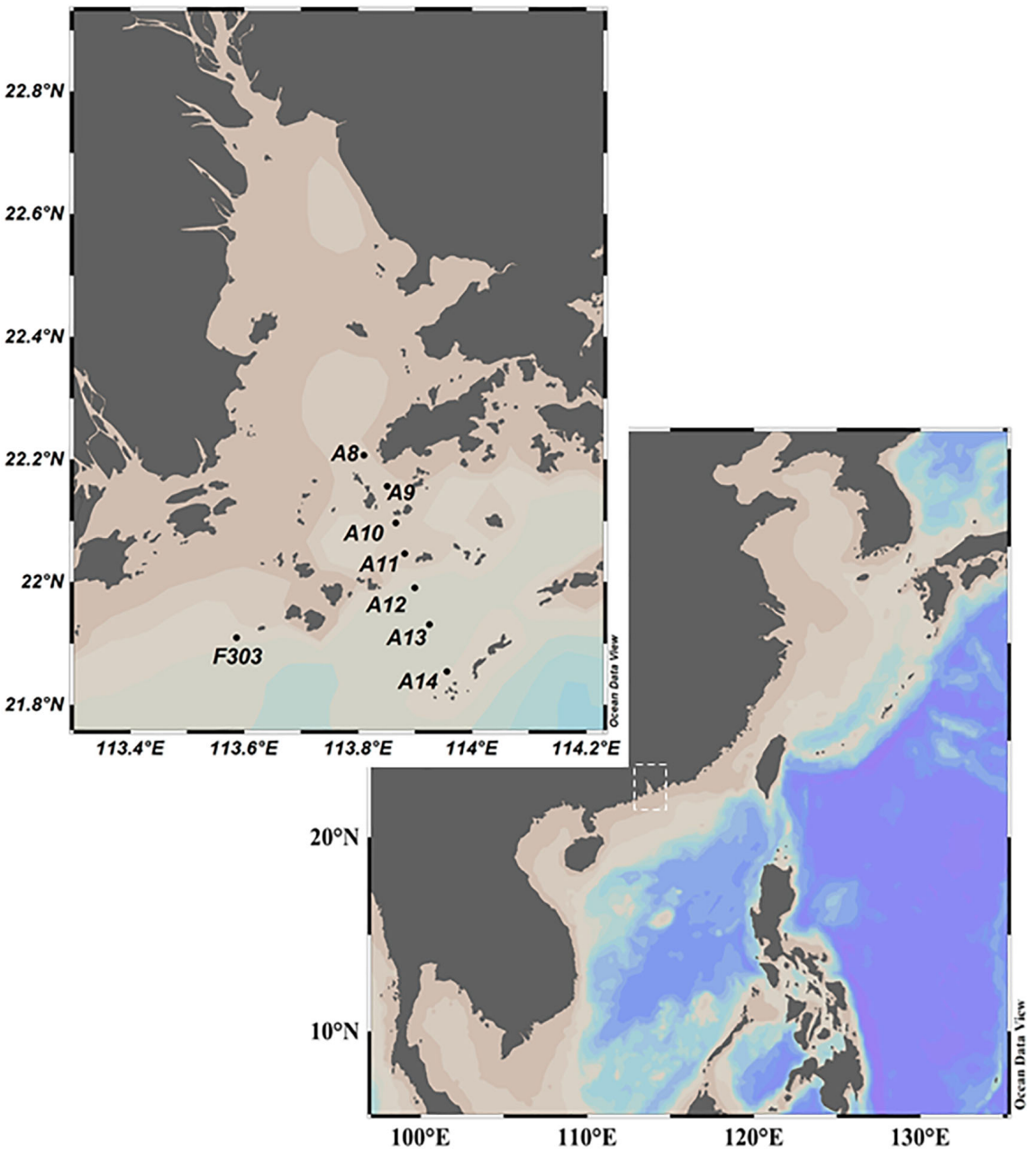

FIGURE 1 | Location of sampling sites on the shelf of the northern South China Sea (NSCS) in July 2018. Figure was produced using Ocean Data View (version 5.1.7).

(n = 14) for $\delta^{13}C$ ratios and a relative standard deviation of 2.9% (n = 13) for concentrations.

Amino Acid Concentrations and $\delta^{13}C$ Values

Amino acid $\delta^{13}C$ ratios were analyzed following a modification (Tang et al., 2017b) of Silfer et al. (1991). Combined AA were released by hydrolyzing filters in 6 N HCl (trace-metal clean, Sigma-Aldrich) for 20 h at 110°C. The hydrolyzate was purified following Takano et al. (2010). Briefly, the hydrolyzate was dried with a stream of N_2 gas, redissolved in 0.1 N HCl, and loaded onto a pipette column that had been packed with Dowex 50WX8 cation exchange resin (Sigma-Aldrich) and preconditioned with 1 N HCl and 1 N NaOH. The column was rinsed with 0.1 N HCl, and then the purified AA were eluted using 1.5 N aqueous ammonium hydroxide. The eluate was dried under N_2, resuspended into acidified isopropanol (20% acetyl chloride), and esterified at 110°C for 1 h. The reaction was stopped by freezing the sample at −20°C. After rinsing with

CH_2Cl_2, samples were acylated with trifluoroacetic anhydride in CH_2Cl_2 at 100°C for 15 min. Ten AAs, alanine (ALA), glycine (GLY), threonine (THR), leucine (LEU), valine (VAL), isoleucine (ILE), proline (PRO), aspartic acid (ASP), glutamic acid (GLU), and phenylalanine (PHE), were separated by gas chromatography (60 m × 0.25 mm, 0.25 μm, HP-5MS) and oxidized to CO_2 online with a combustion oven at 1,000°C. Concentrations of the purified $^{13}CO_2$ and $^{12}CO_2$ were determined by the coupled IRMS (GC-C-IRMS, Thermo Delta V Advantage). The peak of each AA was identified by GC-MS (Pegasus 4D, LECO USA). Norleucine with a known $\delta^{13}C$ value was added to samples before hydrolysis as an internal standard. A mixture of AA standards was derivatized and analyzed in parallel to the samples. The $\delta^{13}C$ ratios of individual AA standards were determined by EA-IRMS. AA concentrations were determined by comparing the peak areas of AA and added norleucine in both samples and external standards as in McCarthy et al. (2013). Triplicate samples were analyzed, and the $\delta^{13}C$ values of AA were corrected for the carbon added during the derivatization process using the external standards. The analytical standard deviation of AA $\delta^{13}C$ values ranged from 0.5 to 1.4‰. A carbon weighted mean of AA $\delta^{13}C$ (*w*AA $\delta^{13}C$) was calculated in a given sample as the sum of individual AA $\delta^{13}C$ value multiplied by its relative carbon molar concentration to total AA carbon molar concentration.

Statistical Analysis

Principal component analysis (PCA) as in Tang et al. (2017a) was applied to normalized AA $\delta^{13}C$ values relative to *w*AA $\delta^{13}C$. The loadings of the first three principal components (PCs) were plotted with the site scores for all the samples measured. The site scores were divided by eight for better visualization. The PCA analysis was carried out using RStudio (version 0.99.902).

Linear discriminant function analysis (LDA) was applied to the $\delta^{13}C$ values of essential AA (ILE, LEU, PHE, THR, and VAL) in shelf particles (Larsen et al., 2013). The data training set came from Larsen et al. (2009, 2013).

The normalized $\delta^{13}C$ values of leucine and isoleucine in shelf particles were linearly regressed using a standardized dataset that included bacteria, forest bacteria, microalgae and open ocean suspended particles following the work by Sabadel et al. (2019).

RESULTS

Input of River Water and Formation of Hypoxia on the NSCS Shelf

A transect across the inner NSCS shelf was surveyed seaward from the mouth of the PRE (station numbers are shown in **Figure 1**). The input of river water was observed in the upper 10 m of most stations with salinity less than 30 (e.g., Stas. A8–A13) (**Figures 2A,B**). More saline waters from the adjacent South China Sea basin clearly occupied bottom waters at more seaward stations (A11–A14). Stratification was much stronger at the seaward end (**Figures 2A,B**), and was also observed at Sta. F303H where freshwater overlies SCS basin water (**Figure 2B**). However, the storm disrupted the stratification, and a well-mixed water column was found when the site was resampled (F303O; **Figures 2A,B**).

Stratification limits the resupply of oxygen from the atmosphere to the bottom of the NSCS shelf, but OC export from the surface continues with subsequent consumption of oxygen during OC decomposition. As a result, lower dissolved oxygen concentrations ranging from 2.0 to 6.5 mg L^{-1} were observed in the mid-depth and bottom water along the transect, in contrast to the saturated surface water (**Figures 2C**, **4B**). The lowest DO was at the bottom of A12, while the highest bottom water DO was at the most seaward station A14, suggesting more exchange of offshore bottom water with open ocean water. The lowest DO concentration of 0.1 mg L^{-1} was found at the bottom of F303H, which is the only surveyed location where hypoxia was observed. This hypoxic bottom water was replenished after the storm (**Figure 2C**). Surface maxima of chl*a* were observed in most stations except the most offshore sta. A14 and sta. F303O after the storm. The highest chl*a* concentrations were in the middle stations of the transect, and they rapidly decreased with depth (A9, A10, and A12; **Figures 2D**, **4A**). The hypoxic station F303H had the lowest chl*a* both before and after the storm.

Distribution of Amino Acid and Bulk Organic Carbon on the NSCS Shelf

The highest particulate organic carbon (POC) concentrations of 100–200 μmol L^{-1} were observed at the nearer shore stations A8 and A9 (**Figure 3A**). These high POC concentrations rapidly decreased seaward. Except for these near shore stations, POC was generally higher in the surface than in the middle and bottom waters. The highest surface POC in the more seaward stations was found at A13, while the lowest was at A14, reflecting the influence of oligotrophic water from the SCS basin.

Particulate AA concentrations ranging from 1.1 to 37.0 μmolC L^{-1} were observed along the surveyed transect (**Figure 3B**). The ratio of AAC/POC was much smaller at Sta. A8–A10 than at more seaward stations (**Supplementary Table 1**).

At more seaward stations (A11–A14), the AA vertical distribution was generally similar to the bulk POC distributions, high at the surface and decreasing with depth. A surface AA maximum of up to 37.0 μmolC L^{-1} at Sta. A13 with the POC maximum there, consistent with a phytoplankton-dominated source of both labile and bulk OC across the shelf. In addition, the AA carbon yield in POC along the transect was lower in nearshore water (2.8%), and increased to 68.1% at the seaward stations (**Supplementary Table 1**). This difference in AA carbon yield is consistent with previous reports of AA carbon yield in the PRE (Chen et al., 2004).

Lower POC and AA concentrations were found at F303 than at the transect stations for both visits to F303 (O and H) (**Figures 3A,B**). The lower POC and AA concentrations were observed at F303O than F303H. The differences in POC and AA between surface and bottom samples were smaller at Sta. F303H, and these differences were even less at F303 after the storm had mixed the entire water column. The AA carbon yield was slightly lower at F303O than at F303H, most likely indicating a decrease in phytoplankton biomass after the storm.

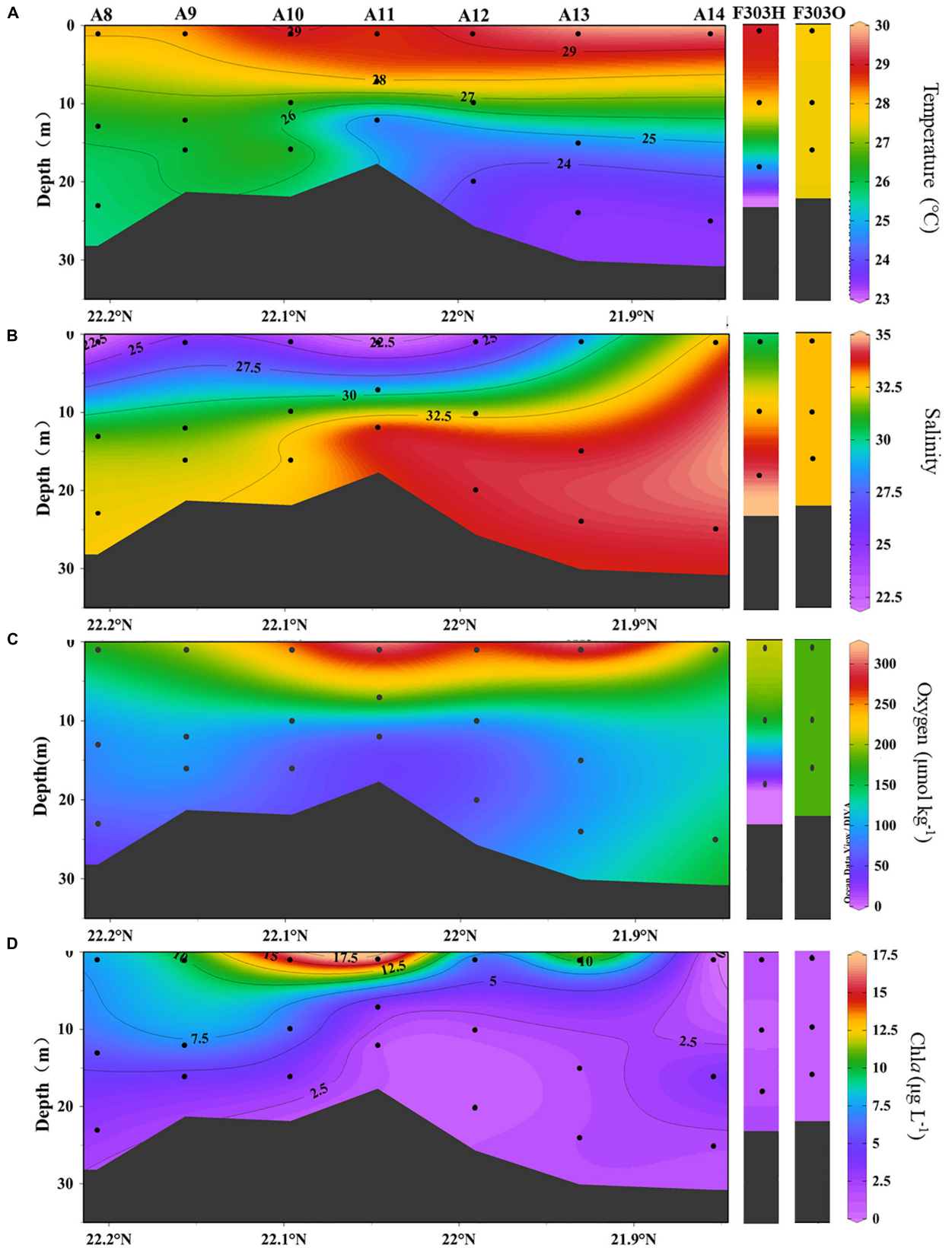

FIGURE 2 | Distribution of **(A)** temperature, **(B)** salinity, **(C)** dissolved oxygen, and **(D)** chl*a* at transect A and station F303 on the NSCS shelf. Station F303H and F303O are the two visits to station F303 before and after Tropical Storm Son-Tinh, respectively.

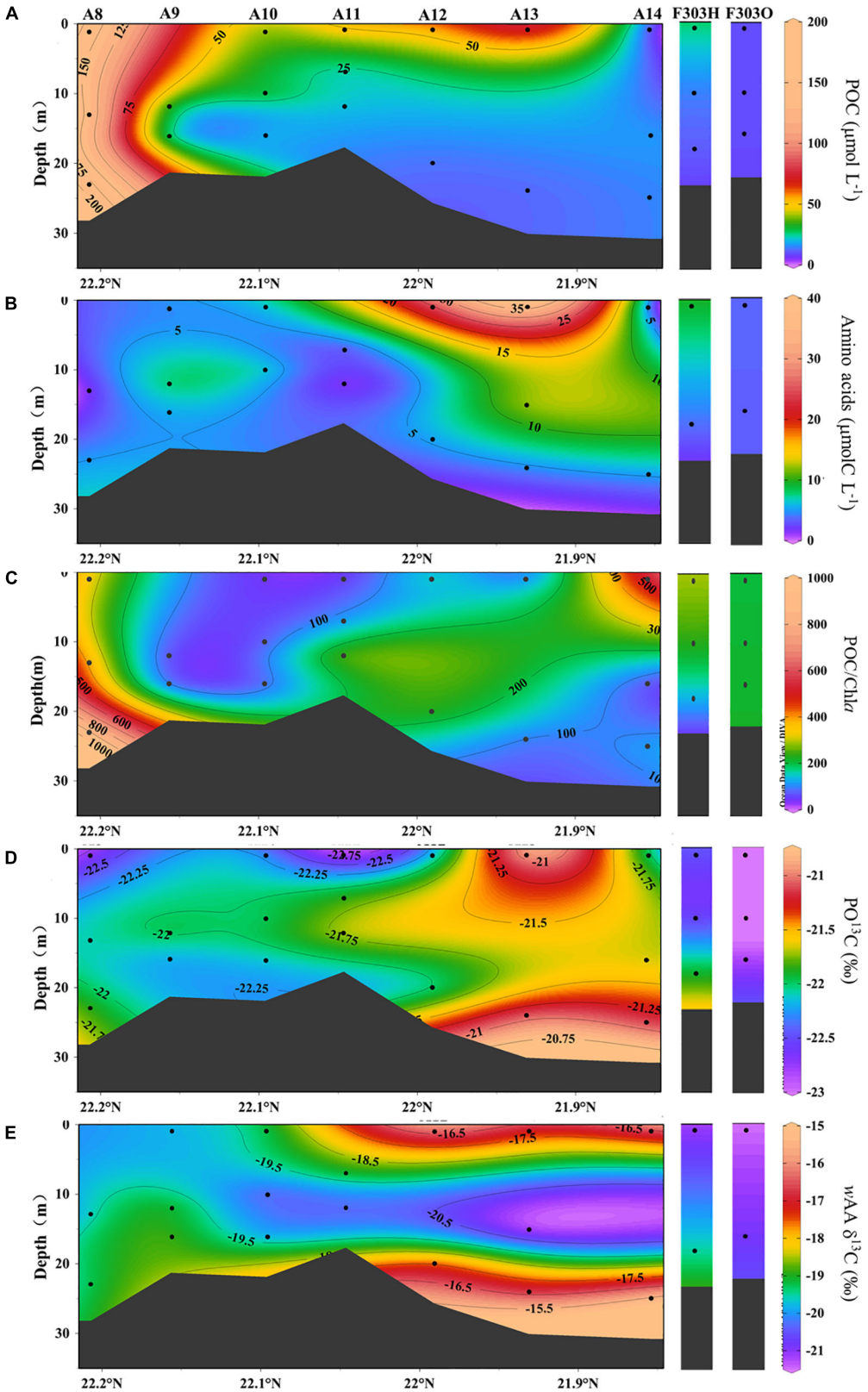

FIGURE 3 | Concentrations of particulate organic carbon **(A)**, amino acids **(B)** and POC/Chl*a* **(C)**, particulate organic carbon $\delta^{13}C$, $PO^{13}C$ **(D)** and carbon-weighted mean of amino acid $\delta^{13}C$, *w*AA $\delta^{13}C$ **(E)** from transect A and station F303 on the NSCS shelf. Station F303H and F303O are the two visits to station F303 before and after Tropical Storm Son-Tinh, respectively.

Distributions of Bulk POC and Amino Acid $\delta^{13}C$

The $\delta^{13}C$ values in POC were relatively constant across all the stations studied, ranging between −23.1 and −21.1‰ (**Figures 3C,D**, **4A,B**). The seaward station $PO^{13}C$ ratios (A12–A14) were somewhat higher than those nearer the coast (A8–A11). This spatial difference among stations was usually larger than the vertical difference between surface and bottom waters at the same station. Carbon-weighted means of AA $\delta^{13}C$ ratios (*w*AA $\delta^{13}C$) ranged from −21.2 to −15.3‰ (**Figures 3D**, **4B**), and were always higher than corresponding $PO^{13}C$ ratios. $PO^{13}C$ and *w*AA $\delta^{13}C$ shared a similar spatial distribution pattern, lower at nearshore stations than at seaward stations. For most stations, surface and bottom particle *w*AA $\delta^{13}C$ ratios were similar, but a slightly lower *w*AA $\delta^{13}C$ was observed at mid-depths.

Individual AA in each sample showed a larger range in $\delta^{13}C$ values, from −30.0‰ in valine to −5.9‰ in glycine. This range agrees with previous reports of AA carbon isotope distribution in estuarine sediments, and both suspended and sinking particles in the open ocean as well as in phytoplankton cells (Keil et al., 2001; McCarthy et al., 2004; Hannides et al., 2013; Larsen et al., 2013, 2015). Among the 10 AAs we studied, isoleucine and leucine showed the least individual variation in $\delta^{13}C$ values, −19.3 ± 1.3‰ and −26.2 ± 1.0‰, respectively (**Figures 4C**, **5A,B**), while valine and glycine showed much larger individual variations, -23.7 ± 4.8‰ and −12.6 ± 3.6‰, respectively (**Figures 4D**, **5C,D**). A decrease in $\delta^{13}C$ value of both LEU and ILE was observed in mid-depth particles of the offshore stations (A10–A12; **Figures 5A,B**). This decrease was not observed in VAL and GLY $\delta^{13}C$; instead, a progressive increase of VAL and GLY $\delta^{13}C$ was observed with depth (**Figures 4D**, **5C,D**).

Although the salinity at F303H/O was somewhat higher than most other stations on the transect, more negative $PO^{13}C$ and *w*AA $\delta^{13}C$ values were observed at F303H/O than at any other stations (**Figures 3C,D**). $PO^{13}C$ and *w*AA $\delta^{13}C$ values were even more negative at F303O than at F303H. Hypoxic bottom water (F303H) has slightly more positive $PO^{13}C$ and *w*AA $\delta^{13}C$ than the overlying surface water. This bottom enrichment in ^{13}C disappeared after the storm (F303O). The ILE $\delta^{13}C$ ratios at F303 decreased slightly after the storm (**Figure 5A**).

Statistical Analysis of Amino Acid $\delta^{13}C$ Values

The first three PCs (PC1, PC2, and PC3) of individual AA normalized $\delta^{13}C$ values ($\delta^{13}C$ values of individual AA relative to *w*AA $\delta^{13}C$ values) for all samples measured are shown in **Figure 6**. PC1, PC2, and PC3 explained 34.6, 17.6, and 12.8% of the variation. LEU had the highest loadings of PC1, while VAL had the lowest loading. Loadings of GLY and GLU were the highest and lowest of PC2, respectively. Loadings of PRO and GLY were the highest and lowest of PC3, respectively. Samples across the NSCS shelf clustered into two groups as seen in **Figure 6A** (PC1 vs PC2): samples from offshore stations clustered at the bottom left, while samples from nearshore stations were at the upper right. In **Figure 6B** (PC1 vs PC3), surface samples (upper) were separated from mid-depth and bottom water samples (bottom). The hypoxic bottom water at Sta. F303 (F303HB) showed no difference from other bottom water samples. Both before and after the storm, Sta. F303H/F303O clustered with the nearshore stations.

DISCUSSION

Source and Recycling of Labile Organic Matter on the NSCS Shelf

Continental shelves and river deltas contain the largest oceanic organic carbon pool found in marine sediments, and 80% of the organic carbon in sediments is buried there (Hedges and Keil, 1995; Gattuso et al., 1998). POC above and on shelf sediments is highly dynamic due to diverse inputs from local primary production and terrestrial sources, exchange with the open ocean, and rapid recycling by water column and benthic micro and macrobiota (Lee and Wakeham, 1988; Bianchi et al., 2013). The POC from these different sources is highly diverse in molecular composition, and has a large span of reactivity and bioavailability (Benner and Amon, 2015). Among the organic compounds on the shelf, labile molecules like AA are most readily recycled (Benner and Amon, 2015). AA, in either particulate or dissolved phase, are widely distributed in coastal areas (e.g., recently by Chen et al., 2004; Liu et al., 2010; Shen et al., 2016; Tang et al., 2017a; Li et al., 2018). The distribution of AA on the shelf is also determined by the sources mentioned above, and the relative abundance of AA to bulk OC varies greatly among the sources (Chen et al., 2004). The removal of shelf AA (and other labile compounds) is usually faster than that of bulk OC because AA degrade faster (Benner and Amon, 2015; Wakeham and Lee, 2019).

Local Primary Production

Hot spots with high dissolved AA concentrations have been found on the coastal shelf of the Gulf of Mexico in response to rapid growth of phytoplankton (Shen et al., 2016). Similarly, on the NSCS shelf, *in situ* primary production can be high, as it is supported by high nutrient inputs from the PRE and from wind driven coastal upwelling (Han et al., 2012). Along our surveyed transect in the summer of 2018, particulate AAs were found to account for up to 68.1% of the bulk POC. This is an even higher percentage than the average cellular content of phytoplankton in estuaries (25–50%; Canuel and Hardison, 2016). The generally higher AA carbon yield across the transect (except at A8) suggests that POC on the NSCS shelf comes mainly from freshly produced phytoplankton, in contrast to terrestrial organic matter or resuspended sediment with its lower AA carbon yield (e.g., A8), as will be discussed later. The vertical decrease in AA and POC concentrations with depth observed at most surveyed stations mirrored the declining chl*a* in the water column. A relatively constant $PO^{13}C$ of −22.0 ± 0.6‰ throughout the surveyed stations agrees with the typical surface $PO^{13}C$ found in the SCS basin (Liu et al., 2007), suggesting that POM on the shelf originates from primary production in seawater.

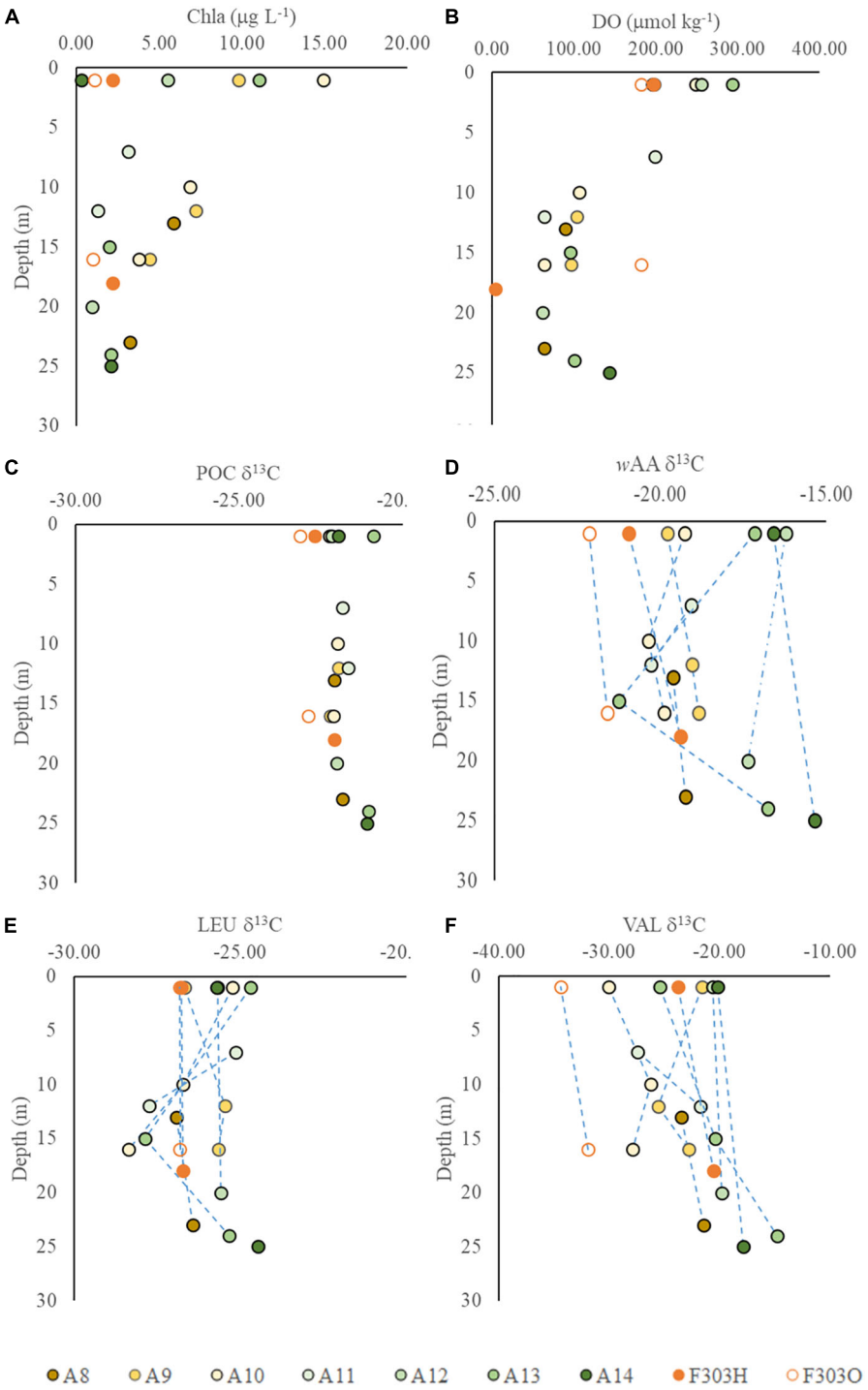

FIGURE 4 | Vertical profiles of $\delta^{13}C$ values in particles from transect A and station F303 on the NSCS shelf: **(A)** Chl*a*; **(B)** DO concentrations; **(C)** particulate organic carbon $\delta^{13}C$, $PO^{13}C$; **(D)** carbon-weighted mean of amino acid $\delta^{13}C$, *w*AA $\delta^{13}C$; **(E)** leucine $\delta^{13}C$; and **(F)** valine $\delta^{13}C$. Station F303H and F303O are the two visits to station F303 before and after Tropical Storm Son-Tinh respectively.

In surface waters of the NSCS shelf, *w*AA$\delta^{13}C$ values varied from −22.2 to −16.2‰, but generally agree with observations of bulk AA $\delta^{13}C$ in phytoplankton (−18.2‰), sinking particles (−16.7‰), and sediment (−17.2 to −19.0‰) from the northeastern Pacific (Wang and Duffel, 1996; Wang et al., 1998), supporting the idea that local primary production is the dominant source of labile organic carbon. Variations in *w*AA$\delta^{13}C$ might be due to either variations in inorganic carbon source

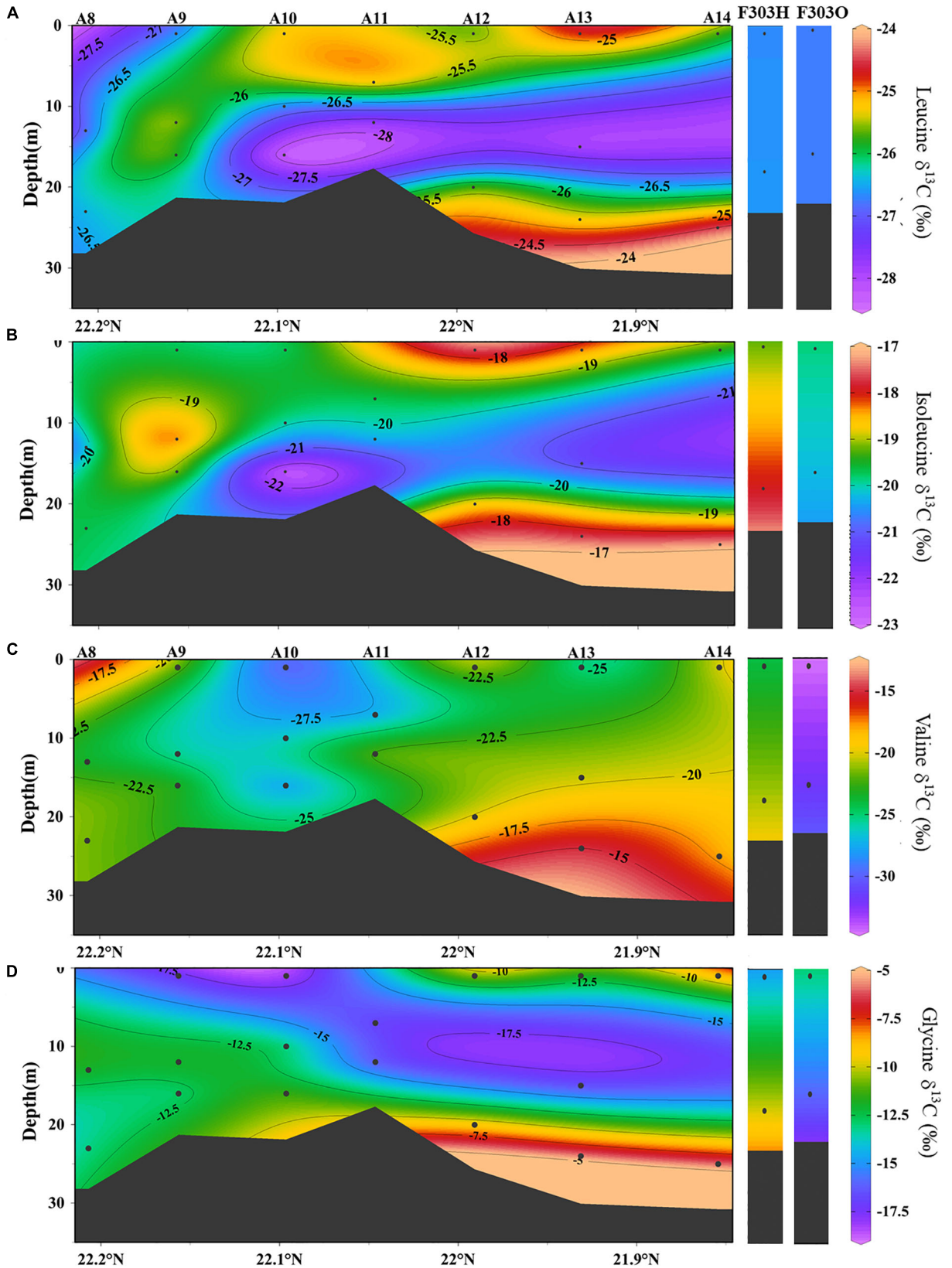

FIGURE 5 | The distribution of $\delta^{13}C$ values in particles from transect A and station F303 on the NSCS shelf: **(A)** leucine $\delta^{13}C$, **(B)** isoleucine $\delta^{13}C$, **(C)** valine $\delta^{13}C$, and **(D)** glycine $\delta^{13}C$. Station F303H and F303O are the two visits to station F303 before and after the Typhon Son-Tinh, respectively.

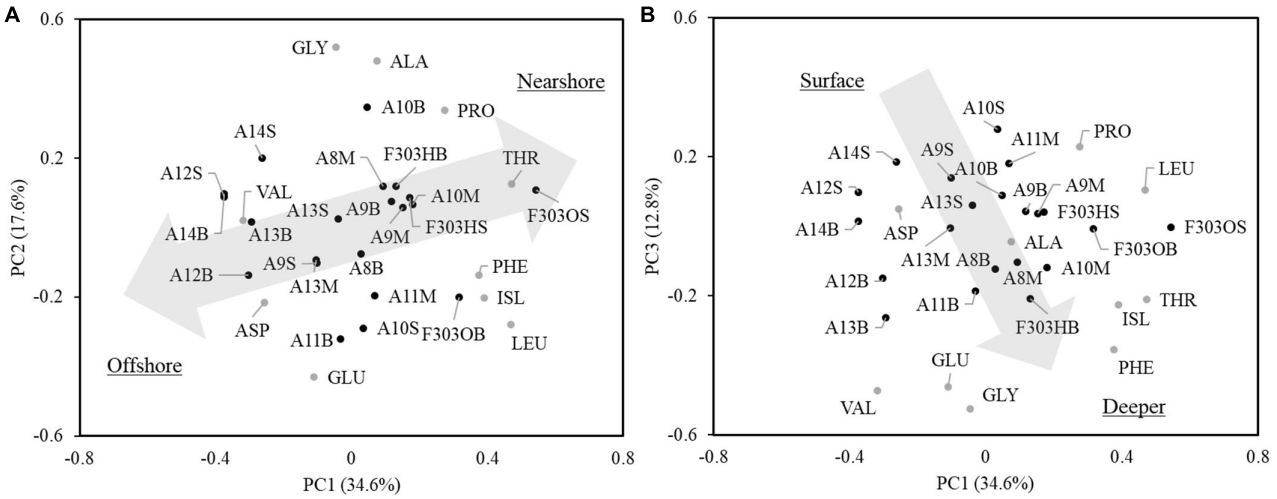

FIGURE 6 | Principal component analysis of amino acid $\delta^{13}C$ values in particles from transect A and station F303. The site scores were divided by eight for better visualization. The first three principal components account for 34.6, 17.6, and 12.8% of the variations. PC1 and PC2 **(A)** clusters the samples into offshore (bottom left) and nearshore (upper right) samples. PC1 and PC3 **(B)** clusters the samples into surface samples (upper) and samples in depth (bottom). Letters behind the station represent depth of the sample, the "S", "M," and "B" indicates surface, middle, and bottom water, respectively. Station F303H and F303O are the two visits to station F303 before and after the Tropical Storm Son-Tinh, respectively.

or isotope fractionation during photosynthesis. A variation of $DI^{13}C$ ranging from −4.0‰ (at A8) to −0.5‰ (at A14) was reported previously on the NSCS shelf in the summer of 2017, with the lowest value at the mouth of the PRE (Zhao et al., 2020). This variation in $DI^{13}C$ ratio might explain the lower *w*AA$\delta^{13}C$ and $PO^{13}C$ in nearshore surface water (F303, A9, A10; **Figure 3**) compared to offshore stations (A12–A14). However, *w*AA $\delta^{13}C$ in offshore surface waters of up to −16.2‰ are even larger than the highest values reported for surface particles of the open ocean (−16.7 to −18.2%; Wang and Duffel, 1996; Wang et al., 1998). These higher values of *w*AA$\delta^{13}C$ in surface particles suggest that the AA $\delta^{13}C$ may also be influenced by isotope fractionation during photosynthesis. Offshore stations had higher AA carbon yields than nearshore stations. It is possible that the elevated AA $\delta^{13}C$ values result from smaller RuBisCo-catalyzed isotope fractionation in more productive shelf surface waters where growth rates are higher (Laws et al., 1995; Popp et al., 1998; Burkhardt et al., 1999). However, phytoplankton growth is inhibited in the open ocean due to a limited supply of nutrients; thus AA $\delta^{13}C$ values in surface waters of the open ocean are lower as RuBisCo-catalyzed isotope fractionations increase (Wang and Duffel, 1996; Wang et al., 1998).

Local primary production could also explain the lower *w*AA$\delta^{13}C$ values in mid-depth waters than those in the surface. Although the nutrient supply was adequate on the shelf, primary production likely decreased with depth due to lower light intensity. As a result, decreased phytoplankton growth rates in the darker mid-depth waters may have led to a change in isotope fractionation (Popp et al., 1998), and a subsequent negative shift in AA $\delta^{13}C$ ratios. *In situ* production may have contributed to some extent to the mid-depth decrease in *w*AA$\delta^{13}C$, but not bottom samples, where diminished photosynthesis is reflected in the low concentration of Chl*a* across the transect.

Isotope ratios of individual compounds reflect not only the inorganic carbon source and the isotope fractionation in photosynthesis, but also the isotope fractionation caused during biosynthesis of individual compounds (Hayes, 2001). The $\delta^{13}C$ values of the total AA and bulk POC are determined by the relative abundance and the $\delta^{13}C$ of the individual molecules present. The $\delta^{13}C$ of individual AA showed different linear relationships with $PO^{13}C$ and had varied slopes (ranging from 0.6373 in ILE to 3.1949 in VAL; **Supplementary Figure 1**), indicating a changing isotope fractionation among individual compounds from the same source (local primary production). This different response of individual AA $\delta^{13}C$ to $PO^{13}C$ agrees with previous findings in algal cultures where isotope fractionations varied among lipid biomarkers from the same species under changing growth rates (Wilkes et al., 2017, 2018). The first two PCs of the PCA cluster the samples surveyed into offshore and nearshore stations (**Figure 6**), supporting the idea that *in situ* primary production is the dominant factor regulating the $\delta^{13}C$ signature of individual AA. This is also supported by the LDA and comparison of normalized leucine and isoleucine (**Figure 7**), where shelf POM clustered with bacteria and microalgae, indicating that shelf AA may predominantly originate from microalgae, and that bacteria may also contribute to the AA $\delta^{13}C$, either by autotrophic carbon fixation, or by heterotrophic decomposition.

A Combined Effect of Lability and Physical Mixing

For many of the bottom samples (A8B, A9M, A9B, A13B, A14B, F303OB, and F303HB), *w*AA$\delta^{13}C$ values were generally similar or slightly more positive than the corresponding surface

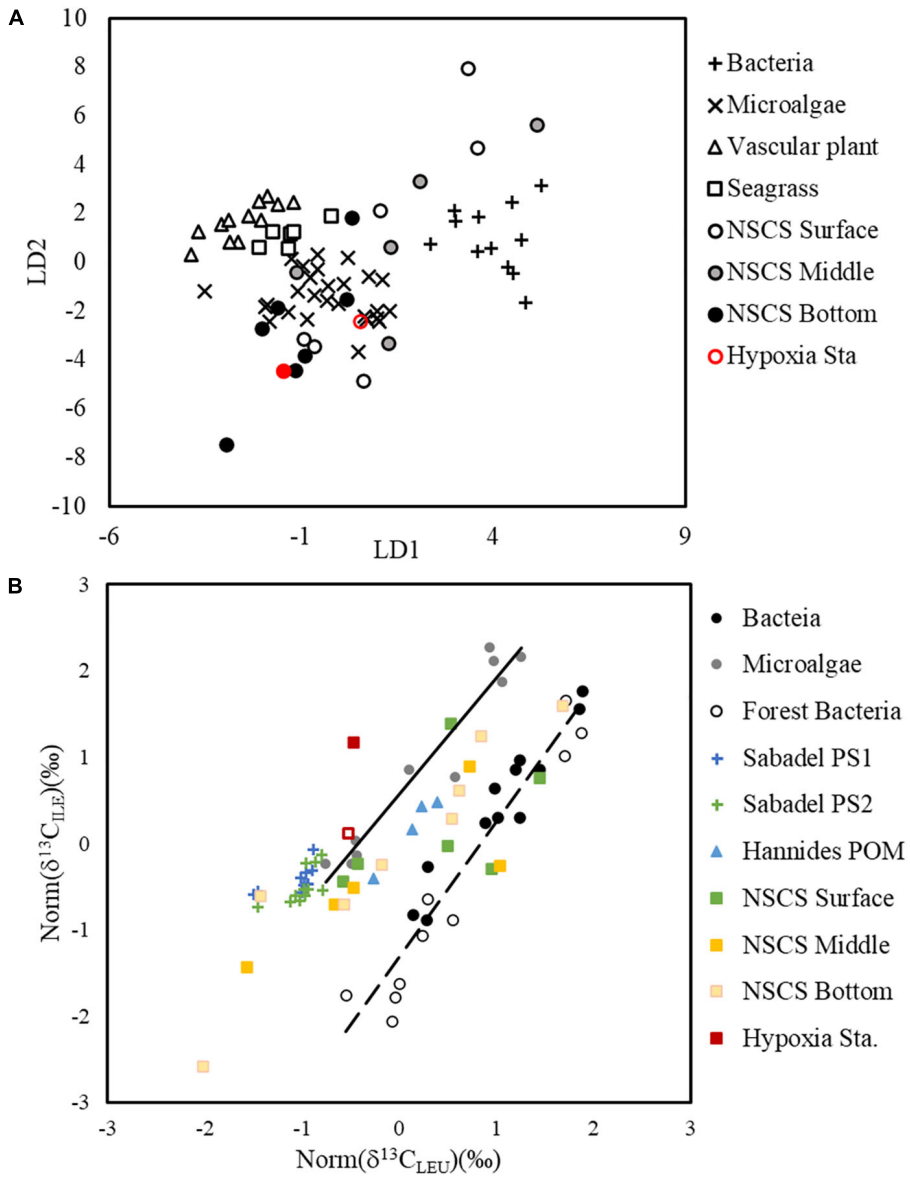

FIGURE 7 | Linear discriminant analysis of essential amino acid $\delta^{13}C$ values from surface, mid-depth, and bottom particles sampled on the NSCS shelf as well as particles from the hypoxic station F303H **(A)**. The training dataset of bacteria, microalgae, vascular plant, and seagrass are from Larsen et al. (2009), Larsen et al. (2013). Normalized $\delta^{13}C$ values of leucine and isoleucine **(B)**. The bacteria (Larsen et al., 2013, 2015), forest bacteria (Larsen et al., 2009), microalgae (Larsen et al., 2013, 2015), Atlantic POM (Sabadel et al., 2019), and Pacific POM (Hannides et al., 2013) were used as a combined dataset for the standardization. The $\delta^{13}C$ values were normalized accordingly in particles from the surface, mid-depth and bottom of the NSCS shelf. The solid and dashed lines are regression lines of microalgae and bacteria.

samples (**Figures 3E**, **4D**). Thus, the *w*AA$\delta^{13}C$ values in the water column showed a spatial variation between nearshore and offshore waters. This *w*AA$\delta^{13}C$ distribution generally follows the transport of two water masses, river input from the nearshore and seawater offshore, respectively (**Figures 1A,B**), indicating physical mixing as the primary forcing regulating the *w*AA$\delta^{13}C$ distribution on NSCS shelf. In contrast to spatial variation of the *w*AA$\delta^{13}C$ across the shelf, $PO^{13}C$ ratios showed a much more constant $\delta^{13}C$ distribution among stations (**Figures 3D**, **4C**). One exception was observed in $PO^{13}C$ at F303O, where a much more negative surface $PO^{13}C$ was observed, which might result from the stronger vertical mixing and increased river discharge after the storm. The different patterns of *w*AA$\delta^{13}C$ and $PO^{13}C$ distributions could result from a number of processes and may be related to a combination of the difference in greater biological lability of AA compared to POC, and also biological and physical processes in this highly dynamic area. As part of labile organic matter, AA are subject to rapid decomposition; thus if AA

are present in the water column, they are probably be more recently produced than the more refractory OM in bulk POC, which has more complicated origins and potentially is more influenced by physical movement. The NSCS shelf around the PRE plume is extensively affected by tides (Dai et al., 2014), which results in diurnal horizontal movement of shelf water. Horizontal transport of suspended particles with tidal movement or other physical processes may contribute to the homogenized $PO^{13}C$ distribution, but less so to AA $\delta^{13}C$, which varies among stations.

Decomposition of POM can also influence the AA isotopic signatures, either by selective remineralization of labile POM to inorganic carbon, and/or degradational modification to other compounds. The influence of bacterial reworking on AA $\delta^{13}C$ in coastal sediment has also been suggested for coastal sediments of phytoplankton origin (Keil et al., 2001), although bulk organic carbon isotopes are thought to be subject to little degradational modification (Freeman, 2001). Because aerobic decomposition consumes oxygen, the extent of decomposition may be partially linked to the DO concentrations in the water column. Along the transect surveyed, lower mid-depth *w*AA$\delta^{13}C$ values (A13M, A12B, A11M, A11B, A10M, and A10B) were found at stations with lower bottom DO concentration (61–105 $\mu mol\ kg^{-1}$) (**Figures 2C**, **4B**), implying that enhanced decomposition may contribute to the decrease of *w*AA$\delta^{13}C$ in these mid-depth particles. This may be due to the selective reworking of certain AA or to the changes in isotopic fractionation during heterotrophic biosynthesis, which is supported by the varied vertical distributions of individual AA $\delta^{13}C$ in the water column (**Figures 4**, **5**). For example, glycine and valine showed increasing $\delta^{13}C$ values from the surface to bottom, while leucine and isoleucine showed decreased $\delta^{13}C$ values in mid-depth (**Figures 4E,F**). However, the influence of decomposition to AA $\delta^{13}C$ is hard to be distinguished from other processes, particularly on this highly dynamic shelf system.

Terrestrial Input and Sediment Resuspension

There is considerable terrestrial input to the NSCS shelf (Dai et al., 2014); the PRE delivers about $3.26 \times 10^{11}\ m^3$ of fresh water (with its associated DOC and POC) to the shelf annually (Cao et al., 2011). In general, river discharge can carry large amounts of terrestrial OM from vascular plant debris and soil leachates (Bianchi, 2011). In addition, studies suggest local phytoplankton production can also be an important contributor of estuarine labile organic components, e.g., fatty acid and Chl*a* (Qian et al., 1996; Bianchi and Bauer, 2011). The rapid turnover of labile components may limit export of this material to the continental shelf. This is supported by a major contribution of local primary production to OM on NSCS shelf based on the carbon isotope signature of POM, sediment OM and DIC (Chen et al., 2008; Zhao et al., 2020). Thus terrestrially derived organic matter may contribute a small proportion to the shelf particulate AA. Differences in *w*AA $\delta^{13}C$ and individual AA $\delta^{13}C$ were observed between nearshore and seaward stations. Based on the first two PCs (**Figure 6**), the samples surveyed roughly cluster into seaward or nearshore samples, but the clusters do not clearly separate from each other. This difference in AA $\delta^{13}C$ may relate more to the $DI^{13}C$ difference between offshore and nearshore stations instead of terrestrial OM input. This is also supported by the constant $PO^{13}C$ values across the transect.

Resuspended sediments can also affect the proportion of labile material reaching shelf sediments. Shallow water depths and highly dynamic water movement can result in resuspending large amounts of sediment OM (accumulated at the sediment-water interface) back to the water column, and this would be greater at nearshore stations. Compared to the particles in the water column, sediment OM is usually older organic matter that is more resistant to further decomposition (Cowie et al., 1995; Wang and Duffel, 1996; Wang et al., 1998; Sheridan et al., 2002). Along the surveyed transect, a mismatch was found between the AA and POC distribution. POC was higher at the most nearshore station (A8), but the AA concentration at A8 was among the lowest measured. This mismatch resulted in a lower AA carbon yield at nearshore stations adjacent to the mouth of the PRE. This may result from either the input of recalcitrant terrestrial OM or resuspension of sediment OM. However, it is difficult to distinguish sediment OM from either terrestrial OM or local primary production due to the complicated origins of sediment OM.

Effect of Coastal Hypoxia on Particulate Organic Carbon

Coastal hypoxia on the NSCS shelf results from the stress of increasing nutrient and terrestrial OM inputs. From June to September, the Southwest monsoon brings 80% of the annual precipitation to the SCS (Su, 2004). As a response, freshwater discharge from the PRE usually reaches a maximum in summer. This high flux of freshwater usually covers the more saline seawater from the SCS basin. Under the influence of these two water masses, the NSCS shelf becomes more stratified in the summer. This stratification is clearly illustrated by the sharp gradient of temperature and salinity with depth at Sta. A10–A12 (**Figures 2A,B**). Continued input of warmer and lower salinity surface water blocks oxygen replenishment of the bottom waters of the NSCS shelf. Hypoxia are formed when this stratification lasts for a longer period of time (Lu et al., 2018), and hypoxia can frequently be observed surrounding the mouth of the PRE at these times. Subtropical summer storms frequently visit the SCS and effectively break up this stratification and resupply the bottom waters with oxygen. Therefore, coastal hypoxia cannot be sustained for a long period of time (usually less than a month) (Qian et al., 2018). However, with increasing inputs of nutrients from the PRE, phytoplankton growth has been gradually increasing (Gan et al., 2010), and has resulted in more frequently observed coastal hypoxia on the NSCS shelf in the summer. At the beginning of our survey, low oxygen bottom water was found to spread around the PRE, with Sta. F303H as the center of hypoxia. This is likely due to the long-lasting stratification driven by calm weather that occurred at that time. The low oxygen bottom water might also have resulted from limited bottom water exchange due to the higher topography in this area. After the tropical storm, the strong wind disturbance

mixed the water column so that all physical and biogeochemical parameters we measured exhibited constant values throughout the water column at F303O.

Although hypoxia is directly related to the loading of OM in the water column, OM from different sources contributes differently to the formation of hypoxia on the NSCS shelf. A major contribution of OM from marine sources was suggested as the major cause of hypoxic water in the lower reaches of the PRE by Su et al. (2017). Our results also support the idea that local primary production is the most likely source of OM driving hypoxia on the NSCS shelf, as seen in the more positive $PO^{13}C$ and $wAA\delta^{13}C$ ratios in the bottom hypoxic water (F303H) compared to those at the surface of F303H and F303O as well as the bottom of F303O. Compared with other nearshore stations (A8–A11), F303 had a higher AA carbon yield, implying that accumulation of labile organic matter may contribute to the rapid consumption of oxygen in hypoxic areas.

A decline in oxygen can influence recycling of shelf OC, particularly labile OC, in two ways. First, labile organic matter can accumulate in the hypoxic bottom water because of increased supply of freshly produced organic matter from the surface, or decreased decomposition in the hypoxic bottom waters, particularly decomposition related to zooplankton consumption (Jessen et al., 2017). Surface AA concentrations at F303 were lower than at the more productive offshore stations (A12, A13). This suggests that OM supply was not the limiting factor for hypoxia to form since primary production was overall very high on the NSCS shelf, while hypoxic waters were found only near Sta. F303. On the other hand, the similar AA carbon yields across the water column might suggest that degradation rates of sinking particles were slower at F303, thus labile OM might accumulate in the bottom waters. Second, the microbial community in low oxygen water probably uses a different metabolic strategy to decompose labile organic matter from that in oxic waters (Liu et al., 2013, 2017). However, if such a metabolic difference occurred at F303H, it does not appear to have influenced individual AA $\delta^{13}C$ values. In the PCA of AA $\delta^{13}C$ (**Figure 6**), hypoxic bottom water at F303H cannot be differentiated from other bottom samples, but is somewhat different from the surface samples. The weak difference between surface samples and bottom samples (**Figure 6**) implies that decompositional modification shifts the AA $\delta^{13}C$ of deeper particles away from the freshly produced surface particles, but this modification did not appear to be influenced by oxygen concentration. This supports findings by Liu et al. (2017) that peptide hydrolysis rates are equally fast in both oxic and hypoxic waters. It is also possible that the short lifetime of most coastal hypoxia events cannot support extensive anaerobic decompositional modification of shelf labile OM $\delta^{13}C$ distributions.

CONCLUSION

Overall, our observations on the NSCS shelf provide new information on the source and recycling of labile organic matter in coastal water under the stress of hypoxia. The $\delta^{13}C$ distribution of AA on the shelf suggests that the labile organic carbon on the NSCS shelf is primarily being regulated by *in situ* production by shelf phytoplankton. Higher $wAA\delta^{13}C$ in offshore water than nearshore might be due to either variations in inorganic carbon source or to isotope fractionation during photosynthesis, both of which are strongly influenced by the physical mixing of river water and offshore seawater. The change of AA $\delta^{13}C$ in the surface particles can be also be observed in the particles beneath the surface water. The contribution of terrestrial input and resuspended sediment to AA may be less important and only limited at the most nearshore stations.

In contrast to the dynamic distribution of $AA\delta^{13}C$, bulk $PO^{13}C$ showed little spatial variation on the NSCS shelf. The different patterns of $AA\delta^{13}C$ and $PO^{13}C$ distribution may result from a combined effect of POM lability and physical processes, which contribute to the homogenized $PO^{13}C$ distribution, but less so to AA $\delta^{13}C$, which varies among stations. Decompositional modification of particles caused a lower wAA $\delta^{13}C$ in some mid-depth particles, although individual AA behaved differently: glycine and valine showed increasing $\delta^{13}C$ from the surface to bottom, while leucine and isoleucine showed lower $\delta^{13}C$ at mid-depth. Our study suggests that the AA $\delta^{13}C$ distribution is better than the bulk POC in distinguishing sources of newly produced organic matter and their recent cycling in the marine environments.

The more positive $PO^{13}C$ and $wAA\delta^{13}C$ values we measured in the bottom hypoxic water (F303H) compared to the water column above or after the storm support the idea that local primary production may be the most likely source of OM driving hypoxia on the NSCS shelf. Based on the comparison of AA $\delta^{13}C$ pattern in oxic and hypoxic waters, it appears that the influence of decomposition may be similar in both the hypoxic and oxic waters we observed on the NSCS shelf.

DATA AVAILABILITY STATEMENT

All datasets generated for this study are included in the article/**Supplementary Material**.

AUTHOR CONTRIBUTIONS

ZY collected and analyzed the samples and prepared the manuscript. HZ set up the analytical method for CSIA analysis. PK helped in sample measurement and data analysis. YZ contributes to the sample collection and provided DO and Chl*a* data. TT organized the experiment and wrote the manuscript. All authors contributed to the article and approved the submitted version.

FUNDING

This work is supported by the National Natural Science Foundation of China (Project Nos. 41976035, 41703070) and the Research Grants Council of the Hong Kong Special Administrative Region, China (Project No. T21-602/16R). This work was presented at a workshop on "Marine Organic Biogeochemistry" (April 2019) funded by the Deutsche

Forschungsgemeinschaft (DFG project number 422798570) and the Hanse-Wissenschaftskolleg, and the Geochemical Society.

ACKNOWLEDGMENTS

We thank J. Li, K. Uthaipan, Z. Q. Liu, Z. M. Lu, and D. Li for sample collection. We appreciate H. B. Liu to provide the Chl*a* data. We thank L. Tian and W. B. Zou for assistance with EA-IRMS analysis. Y. Y. Li and X. H. Wang for assistance with GC-MS analysis. We thank C. Lee and Z. Q. Liu for their help in reviewing the manuscript. We appreciate the help of the captain and crew of R/V Haike 68.

SUPPLEMENTARY MATERIAL

The Supplementary Material for this article can be found online at: https://www.frontiersin.org/articles/10.3389/fmars.2020.00675/full#supplementary-material

REFERENCES

Benner, R., and Amon, R. M. W. (2015). The size-reactivity continuum of major bioelements in the Ocean. *Ann. Rev. Mar. Sci.* 7, 185–205. doi: 10.1146/annurev-marine-010213-135126

Bianchi, T., Allison, M., and Cai, W. (eds) (2013). *Biogeochemical Dynamics at Major River-Coastal Interfaces: Linkages With Global Change*. Cambridge: Cambridge University Press, doi: 10.1017/CBO9781139136853

Bianchi, T. S. (2011). The role of terrestrially derived organic carbon in the coastal ocean: a changing paradigm and the priming effect. *Proc. Natl. Acad. Sci. U.S.A.* 108, 19473–19481. doi: 10.1073/pnas.1017982108

Bianchi, T. S., and Bauer, J. E. (2011). Particulate organic carbon cycling and transformation. *Treat. Estuar. Coast. Sci.* 5, 67–117. doi: 10.1016/B978-0-12-374711-2.00503-9

Breitburg, D., Levin, L. A., Oschlies, A., Grégoire, M., Chavez, F. P., Conley, D. J., et al. (2018). Declining oxygen in the global ocean and coastal waters. *Science* 359:eaam7240. doi: 10.1126/science.aam7240

Burkhardt, S., Riebesell, U., and Zondervan, I. (1999). Effects of growth rate, CO2 concentration, and cell size on the stable carbon isotope fractionation in marine phytoplankton. *Geochim. Cosmochim. Acta* 63, 3729–3741. doi: 10.1016/s0016-7037(99)00217-3

Canuel, E. A., and Hardison, A. K. (2016). Sources, ages, and alteration of organic matter in estuaries. *Ann. Rev. Mar. Sci.* 8, 409–434. doi: 10.1146/annurev-marine-122414-034058

Cao, Z., Dai, M., Zheng, N., Wang, D., Li, Q., Zhai, W., et al. (2011). Dynamics of the carbonate system in a large continental shelf system under the influence of both a river plume and coastal upwelling. *J. Geophys. Res. Biogeosci.* 116, 1–14. doi: 10.1029/2010JG001596

Chen, F., Zhang, L., Yang, Y., and Zhang, D. (2008). Chemical and isotopic alteration of organic matter during early diagenesis: evidence from the coastal area off-shore the Pearl River estuary, south China. *J. Mar. Syst.* 74, 372–380. doi: 10.1016/j.jmarsys.2008.02.004

Chen, J., Li, Y., Yin, K., and Jin, H. (2004). Amino acids in the Pearl River Estuary and adjacent waters: Origins, transformation and degradation. *Cont. Shelf Res.* 24, 1877–1894. doi: 10.1016/j.csr.2004.06.013

Close, H. G. (2019). Compound-specific isotope geochemistry in the ocean. *Ann. Rev. Mar. Sci.* 11, 10.1–10.30. doi: 10.1146/annurev-marine-121916-063634

Cowie, G. L., Hedges, J. I., Prahl, F. G., and de Lance, G. J. (1995). Elemental and major biochemical changes across an oxidation front in a relict turbidite: An oxygen effect. *Geochim. Cosmochim. Acta* 59, 33–46. doi: 10.1016/0016-7037(94)00329-k

Dai, M., Gan, J. P., Han, A., Kung, H. S., and Yin, Z. (2014). "Physical dynamics and biogeochemistry of the Pearl River plume," in *Biogeochemical Dynamics at Major River-Coastal Interfaces: Linkages with Global Change*, eds T. Bianchi, M. Allison, and W.-J. Cai (Cambridge: Cambridge University Press), 321–352. doi: 10.1017/cbo9781139136853.017

Freeman, K. H. (2001). "Isotopic biogeochemistry of marine organic carbon," in *Stable Isotope Geochemistry*, *Reviews in Mineralogy and Geochemistry*, Vol. 43, eds J. W. Valley and D. R. Cole (Berlin: De Gruyter), 579–605. doi: 10.2138/gsrmg.43.1.579

Gan, J., Lu, Z., Dai, M., Cheung, A. Y. Y., Liu, H., and Harrison, P. (2010). Biological response to intensified upwelling and to a river plume in the northeastern South China Sea: a modeling study. *J. Geophys. Res. Ocean* 115, 1–19. doi: 10.1029/2009JC005569

Gattuso, J. P., Frankignoulle, M., and Wollast, R. (1998). Carbon and carbonate metabolism in coastal aquatic ecosystems. *Annu. Rev. Ecol. Syst.* 29, 405–434. doi: 10.1146/annurev.ecolsys.29.1.405

Han, A., Dai, M., Kao, S., Gan, J., Li, Q., Wang, L., et al. (2012). Nutrient dynamics and biological consumption in a large continental shelf system under the influence of both a river plume and coastal upwelling. *Limnol. Oceanogr.* 57, 486–502. doi: 10.4319/lo.2012.57.2.0486

Hannides, C. C. S., Popp, B. N., AnelaChoy, C., and Drazen, J. C. (2013). Midwater zooplankton and suspended particle dynamics in the North Pacific Subtropical Gyre: a stable isotope perspective. *Limnol. Oceanogr.* 58, 1931–1936. doi: 10.4319/lo.2013.58.6.1931

Hayes, J. M. (2001). Fractionation of carbon and hydrogen isotopes in biosynthetic processes. *Rev. Mineral. Geochemistry* 43, 225–277. doi: 10.2138/gsrmg.43.1.225

Hedges, J. I., and Keil, R. G. (1995). Sedimentary organic matter preservation: an assessment and speculative synthesis. *Mar. Chem.* 49, 81–115. doi: 10.1016/0304-4203(95)00008-F

Jessen, G. L., Lichtschlag, A., Ramette, A., Pantoja, S., Rossel, P. E., Schubert, C. J., et al. (2017). Hypoxia causes preservation of labile organic matter and changes seafloor microbial community composition (Black Sea). *Sci. Adv.* 3:e1601897. doi: 10.1126/sciadv.1601897

Kao, S. J., Terence Yang, J. Y., Liu, K. K., Dai, M., Chou, W. C., Lin, H. L., et al. (2012). Isotope constraints on particulate nitrogen source and dynamics in the upper water column of the oligotrophic South China Sea. *Global. Biogeochem. Cycles* 26:GB2033. doi: 10.1029/2011gb004091

Keil, R. G., Fogel, M. L., Keill, R. G., and Fogel, L. (2001). Reworking of amino acid in marine sediments: stable carbon isotopic composition of amino acids in sediments along the Washington Coast *Limnol. Oceanogr.* 46, 14–23. doi: 10.4319/lo.2001.46.1.0014

Kemp, W. M., Sampou, P. A., Garber, J., Tuttle, J., and Boynton, W. R. (1992). Seasonal depletion of oxygen from bottom waters of Chesapeake Bay: roles of benthic and planktonic respiration and physical exchange processes. *Mar. Ecol. Prog. Ser.* 85, 137–152. doi: 10.2307/24829928

Larsen, T., Kiel, C., Bach, L. T., Wang, Y. V., Kiel, C., Ventura, M., et al. (2015). Assessing the potential of amino acid 13C patterns as a carbon source tracer in marine sediments: effects of algal growth conditions and sedimentary diagenesis. *Biogeosciences* 12, 4979–4992. doi: 10.5194/bg-12-4979-2015

Larsen, T., Taylor, D. L., Leigh, M. B., and O'Brien, D. M. (2009). Stable isotope fingerprinting: a novel method for identifying plant, fungal, or bacterial origins of amino acids. *Ecology* 90, 3526–3535. doi: 10.1890/08-1695.1

Larsen, T., Ventura, M., Andersen, N., O'Brien, D. M., Piatkowski, U., and McCarthy, M. D. (2013). Tracing carbon sources through aquatic and terrestrial food webs using amino acid stable isotope fingerprinting. *PLoS One* 8:e73441. doi: 10.1371/journal.pone.0073441

Laws, E. A., Popp, B. N., Bidigare, J. R. R., Kennicutt, M. C., and Macko, S. A. (1995). Dependence of phytoplankton carbon isotopic composition on growth rate and [CO2]aq: theoretical considerations and experimental results. *Geochim. Cosmochim. Acta* 59, 1131–1138. doi: 10.1016/0016-7037(95)00030-4

Lee, C., and Wakeham, S. G. (1988). "Organic matter in seawater: Biogeochemical processes," in *Chemical Oceanography*, Vol. 9, ed. J. P. Riley (Cambridge, MA: Academic Press), 1–51.

Li, X., Liu, Z., Chen, W., Wang, L., He, B., Wu, K., et al. (2018). Production and transformation of dissolved and particulate organic matter as indicated by

amino acids in the Pearl River Estuary. *China. J. Geophys. Res. Biogeosci.* 123, 1–15. doi: 10.1029/2018JG004690

Liu, K. K., Kao, S. J., Hu, H. C., Chou, W. C., Hung, G. W., and Tseng, C. M. (2007). Carbon isotopic composition of suspended and sinking particulate organic matter in the northern South China Sea-From production to deposition. *Deep. Res. Part II* 54, 1504–1527. doi: 10.1016/j.dsr2.2007.05.010

Liu, S., Wawrik, B., and Liu, Z. (2017). Different bacterial communities involved in peptide decomposition between normoxic and hypoxic coastal waters. *Front. Microbiol.* 8:353. doi: :10.3389/fmicb.2017.00353

Liu, Z., Kobiela, M. E., McKee, G. A., Tang, T., Lee, C., Mulholland, M. R., et al. (2010). The effect of chemical structure on the hydrolysis of tetrapeptides along a river-to-ocean transect: AVFA and SWGA. *Mar. Chem.* 119, 108–120. doi: 10.1016/j.marchem.2010.01.005

Liu, Z., Liu, S., Liu, J., and Gardner, W. S. (2013). Differences in peptide decomposition rates and pathways between hypoxic and oxic coastal environments. *Mar. Chem.* 157, 67–77. doi: 10.3389/fmicb.2017.00353

Lu, Z., Gan, J., Dai, M., Liu, H., and Zhao, X. (2018). Joint effects of extrinsic biophysical fluxes and intrinsic hydrodynamics on the formation of hypoxia west off the Pearl River estuary. *J. Geophys. Res. C Ocean* 123, 6241–6259. doi: 10.1029/2018JC014199

McCarthy, M. D., Benner, R., Lee, C., Hedges, J. I., and Fogel, M. L. (2004). Amino acid carbon isotopic fractionation patterns in oceanic dissolved organic matter: an unaltered photoautotrophic source for dissolved organic nitrogen in the ocean? *Mar. Chem.* 92, 123–134. doi: 10.1016/j.marchem.2004.06.021

McCarthy, M. D., Lehman, J., and Kudela, R. (2013). Compound-specific amino acid δ15N patterns in marine algae: tracer potential for cyanobacterial vs. eukaryotic organic nitrogen sources in the ocean. *Geochim. Cosmochim. Acta* 103, 104–120. doi: 10.1016/j.gca.2012.10.037

Pai, S. C., Gong, G. C., and Liu, K. K. (1993). Determination of dissolved oxygen in seawater by direct spectrophotometry of total iodine. *Mar. Chem.* 41, 343–351. doi: 10.1016/0304-4203(93)90266-q

Popp, B. N., Laws, E. A., Bidigare, R. R., Dore, J. E., Hanson, K. L., and Wakeham, S. G. (1998). Effect of phytoplankton cell geometry on carbon isotopic fractionation. *Geochim. Cosmochim. Acta* 62, 69–77. doi: 10.1016/s0016-7037(97)00333-5

Qian, W., Gan, J., Liu, J., He, B., Lu, Z., Guo, X., et al. (2018). Current status of emerging hypoxia in a eutrophic estuary: the lower reach of the Pearl River Estuary. *China. Estuar. Coast. Shelf Sci.* 205, 58–67. doi: 10.1016/j.ecss.2018.03.004

Qian, Y., Kennicutt, M. C., Svalberg, J., Macko, S. A., Bidigare, R. R., and Walker, J. (1996). Suspended particulate organic matter (SPOM) in Gulf of Mexico estuaries: Compound-specific isotope analysis and plant pigment compositions. *Org. Geochem.* 24, 875–888. doi: 10.1016/S0146-6380(96)00072-1

Rabalais, N. N., Cai, W.-J., Carstensen, J., Conley, D. J., Fry, B., Hu, X., et al. (2014). Eutrophication-driven deoxygenation in the coastal ocean. *Oceanography* 27, 172–183. doi: 10.5670/oceanog.2014.21

Sabadel, A. J. M., Van Oostende, N., Ward, B. B., Woodward, E. M. S., Van Hale, R., and Frew, R. D. (2019). Characterization of particulate organic matter cycling during a summer North Atlantic phytoplankton bloom using amino acid C and N stable isotopes. *Mar. Chem.* 214:103670. doi: 10.1016/j.marchem.2019.103670

Shen, Y., Fichot, C. G., Liang, S. K., Benner, R., Fichot, G., Liang, S. K., et al. (2016). Biological hot spots and the accumulation of marine dissolved organic matter in a highly productive ocean margin. *Limnol. Oceanogr.* 61, 1287–1300. doi: 10.5670/oceanog.2014.21

Sheridan, C. C., Lee, C., Wakeham, S. G., and Bishop, J. K. B. (2002). Suspended particle organic composition and cycling in surface and midwaters of the equatorial Pacific Ocean. *Deep Sea Res. Part I* 49, 1983–2008. doi: 10.1016/s0967-0637(02)00118-8

Silfer, J. A., Engel, M. H., Limited, V. G. I., Way, A., and Oht, C. C. (1991). Stable carbon isotope analysis of amino acid enantiomers by conventional isotope ratio mass spectrometry and combined gas chromatography isotope ratio mass spectrometry. *Anal. Chem.* 63, 370–374. doi: 10.1021/ac00004a014

Su, J. (2004). Overview of the South China Sea circulation and its influence on the coastal physical oceanography outside the Pearl River Estuary. *Cont. Shelf Res.* 24, 1745–1760. doi: 10.1016/j.csr.2004.06.005

Su, J., Dai, M., He, B., Wang, L., Gan, J., Guo, X., et al. (2017). Tracing the origin of the oxygen-consuming organic matter in the hypoxic zone in a large eutrophic estuary: The lower reach of the Pearl River Estuary, China. *Biogeosciences* 14, 4085–4099. doi: 10.5194/bg-14-4085-2017

Takano, Y., Kashiyama, Y., Ogawa, N. O., Chikaraishi, Y., and Ohkouchi, N. (2010). Isolation and desalting with cation-exchange chromatography for compound-specific nitrogen isotope analysis of amino acids: application to biogeochemical samples. *Rapid Commun. Mass Spectrom.* 24, 2317–2323. doi: 10.1002/rcm.4651

Tang, T., Filippino, K. C., Liu, Z., Mulholland, M. R., and Lee, C. (2017a). Peptide hydrolysis and uptake of peptide hydrolysis products in the James River estuary and lower Chesapeake Bay. *Mar. Chem.* 197, 52–63. doi: 10.1016/j.marchem.2017.10.002

Tang, T., Mohr, W., Sattin, S. R., Rogers, D. R., Girguis, P. R., and Pearson, A. (2017b). Geochemically distinct carbon isotope distributions in *Allochromatium vinosum* DSM 180 T grown photoautotrophically and photoheterotrophically. *Geobiology* 15, 324–339. doi: 10.1111/gbi.12221

Wakeham, S. G., and Lee, C. (2019). Limits of our knowledge, part 2: Selected frontiers in marine organic biogeochemistry. *Mar. Chem.* 212, 16–46. doi: 10.1016/j.marchem.2019.02.005

Wakeham, S. G., Lee, C., Hedges, J. I., Hernes, P. J., and Peterson, M. L. J. (1997). Molecular indicators of diagenetic status in marine organic matter. *Geochim. Cosmochim. Acta* 61, 5363–5369. doi: 10.1016/S0016-7037(97)00312-8

Wang, X., and Duffel, E. R. M. (1996). Radiocarbon in organic compound classes in particulate organic matter and sediment in the deep northeast Pacific Ocean. *Geophys. Res. Lett.* 23, 3583–3586. doi: 10.1029/96gl03423

Wang, X. C., Druffel, E. R. M., Griffin, S., Lee, C., and Kashgarian, M. (1998). Radiocarbon studies of organic compound classes in plankton and sediment of the northeastern Pacific Ocean. *Geochim. Cosmochim. Acta* 62, 1365–1378. doi: 10.1016/S0016-7037(98)00074-X

Wilkes, E. B., Carter, S. J., and Pearson, A. (2017). CO2 -dependent carbon isotope fractionation in the dinoflagellate *Alexandrium tamarense*. *Geochim. Cosmochim. Acta* 212, 48–61. doi: 10.1016/j.gca.2017.05.037

Wilkes, E. B., Lee, R. B. Y., McClelland, H. L. O., Rickaby, R. E. M., and Pearson, A. (2018). Carbon isotope ratios of coccolith–associated polysaccharides of Emiliania huxleyi as a function of growth rate and CO2 concentration. *Org. Geochem.* 119, 1–10. doi: 10.1016/j.orggeochem.2018.02.006

Zhang, H., and Li, S. (2010). Effects of physical and biochemical processes on the dissolved oxygen budget for the Pearl River Estuary during summer. *J. Mar. Syst.* 79, 65–88. doi: 10.1016/j.jmarsys.2009.07.002

Zhao, Y., Liu, J., Uthaipan, K., Song, X., Xu, Y., He, B., et al. (2020). Dynamics of inorganic carbon and pH in a large subtropical continental shelf system: Interaction between eutrophication, hypoxia, and ocean acidification. *Limnol. Oceanogr.* 65, 1359–1379. doi: 10.1002/lno.11393

Conflict of Interest: The authors declare that the research was conducted in the absence of any commercial or financial relationships that could be construed as a potential conflict of interest.